CHAPTER V

EXPERIMENTAL INVESTIGATION USING SMALL-SCALE TESTS

5.1 General

According to the numerical investigation of axle loads identification explained in chapter IV, the obtained results reveal that the axle loads of moving vehicle can be accurately identified using the bridge moments. However, for the real B-WIM application, it is known that the real bridge and vehicle are much more complex so that the computer model might not be preciously represented. Therefore, the investigation on full-scale model of vehicle-bridge system is of interest. Unfortunately, although the identification results obtained actual full-scale bridge tests are the most reliable method of investigation. It is very expensive and only limited number of tested conditions can be conducted. In this chapter, the experimental investigation on axle loads identification using small-scale model is considered. By varying the vehicle's weights, speeds, axle spacing and its travelling paths, the effectiveness of the two identification methods are determined and discussed.

5.2 Experimental Setup

The small-scale bridge is firstly designed based on the vibration characteristics of an actual bridge. The fundamental frequency of the bridge is used as the target design parameter. Then the vehicle model is designed accordingly to conform with the order of actual bridge responses as occurred in practice. The scaled dimensions of both the bridge and the vehicle can be determined from their physical characteristic such as axle spacings to span ratios and durations of travel with respect to the actual situations. (Asanachinda, 2008).

The experimental setup of the small-scale bridge and vehicle are diagrammatically shown in Figures 5.1(a) to 5.1(d). The deck of the bridge model is made of a rectangular steel plate having a uniform thickness of 200cm x 50cm x 1cm and is divided into 3 spans consisting of leading span, main span and trailing span. The leading span is used for the vehicle to increase its speed before approaching the

bridge. The trailing span is used to stop the moving vehicle after leaving the bridge. Since the deck of the main span is well separated from two side spans, it is treated as a simply supported bridge. The travel path of the vehicle is controlled by aluminum guide rails attached to the scaled bridge deck. Three guide rails are attached at the quarter points to allow for three different vehicle paths. The vehicle model having two axles with spacing of 28 cm and two rubber wheels for each axle is employed. The vehicle is pulled along the bridge with string. In order to measure positions of the vehicle, the black/white optical detection sensors are installed on the vehicle and the bridge deck.

The bending moments of the bridge at three sections, i.e. at $L/3$, $L/2$ and $2L/3$, are measured. To do so, nine strain gauges are attached beneath the bridge at equal spacing for each bridge section. In order to measure dynamic axle loads of the vehicle, the four strain gauges are installed at its suspension arms. Based on the load calibration with strain readings, the time histories of the axle loads can be directly obtained from the strain measurement. In addition, the vehicle is equipped with black/white optical detection sensors to record positions that the vehicle model has passed as a function of time. By counting pulses from black and white strips reading, the vehicle position as well as the corresponding speed can be determined. For all installations, twenty seven strain gauges at three bridge sections, four strain gauges at the vehicle suspensions, and one optical sensor are all connected to the data acquisition and are simultaneously recorded using the control computer. Data acquisition is completed with a 48 channel logger set at a sampling rate of 1024 Hz for all 32 connected sensors. Every strain gauges and optical sensor are all connected through completion bridge boxes and are simultaneously convert the measured analog signals to the corresponding digital signals by the 32 bits A/D converter before transmitting them to the data logger. Figure 5.2 shows photographs of the instruments used in this experiment. The optical sensor used in detecting vehicle location has 2 infrared sensors, one for a signal emission while another is for a signal receiver. Based on the light that reflected and absorbed by the black-white tape alternately placed with constant stripes width, the optical sensor records data with constant values of 0 and 1.0 when it reads the black and white stripes respectively as shown in Figure 5.3.

The sampling rate of the data acquisition system of 1024 Hz is used for all tests in order to get the highest quality of the recorded signals before filtering. To

reduce the number of data points used for identification as well as the measurement noises imposed in the measured signals, the moving averaging technique with re-sampling of 256 Hz is employed.

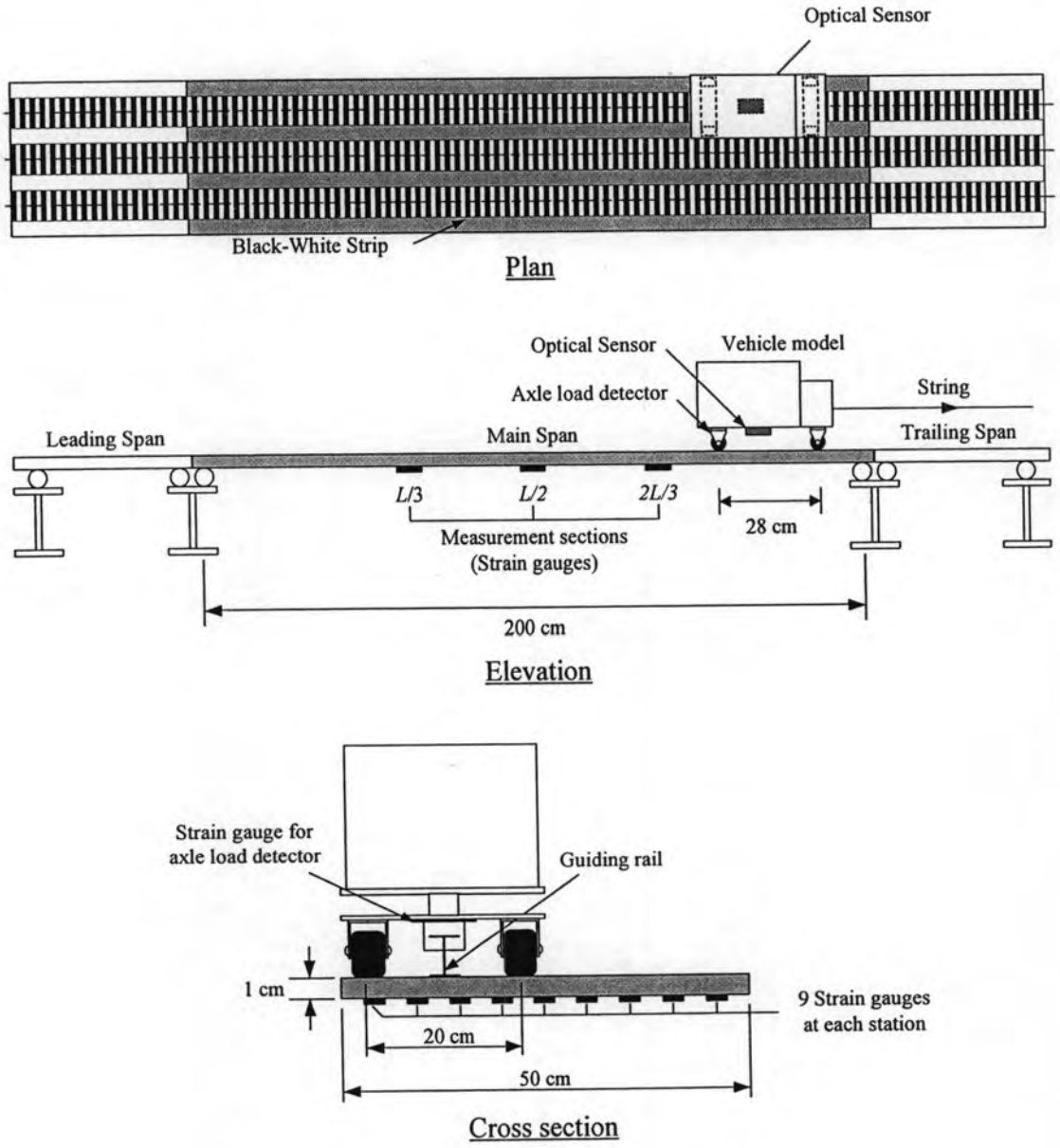

Figure 5.1(a) Set-up for experimental test

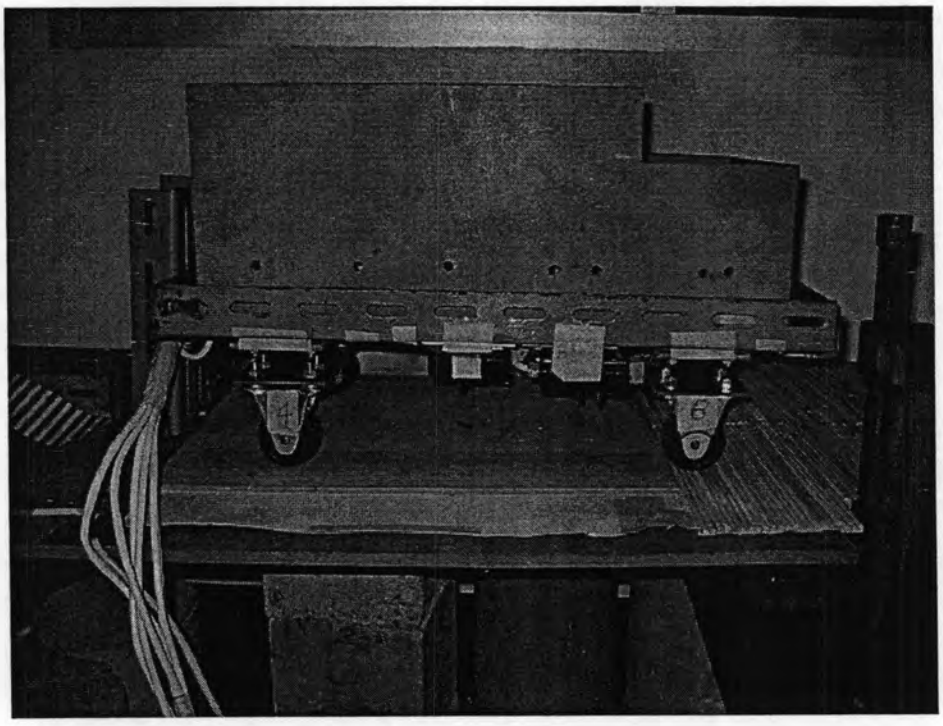

Figure 5.1(b) 2-axle vehicle model

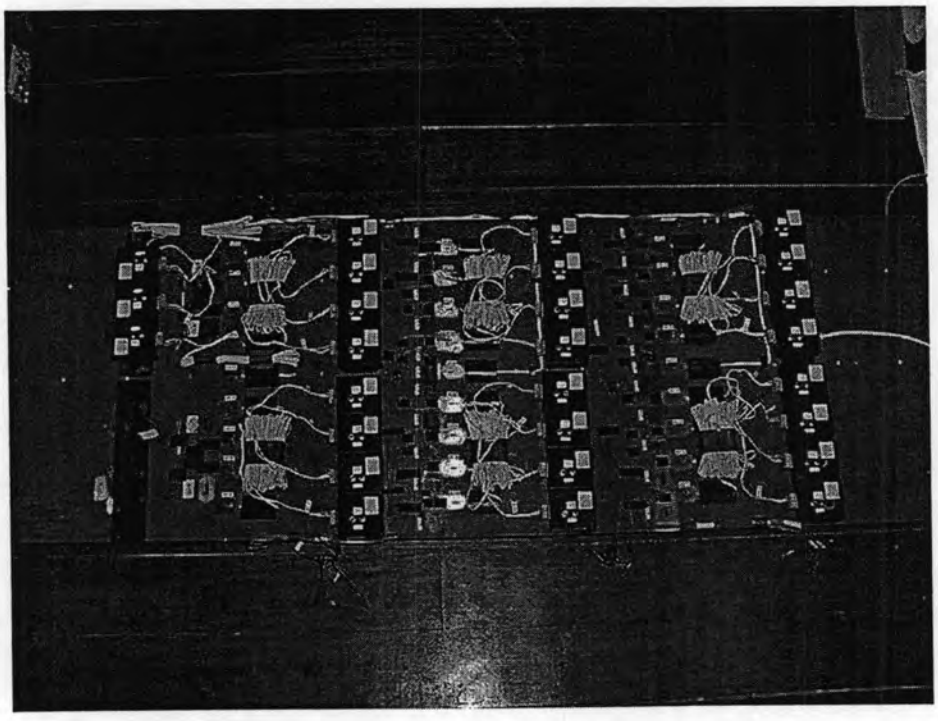

Figure 5.1(c) Strain gauges installation beneath the bridge deck

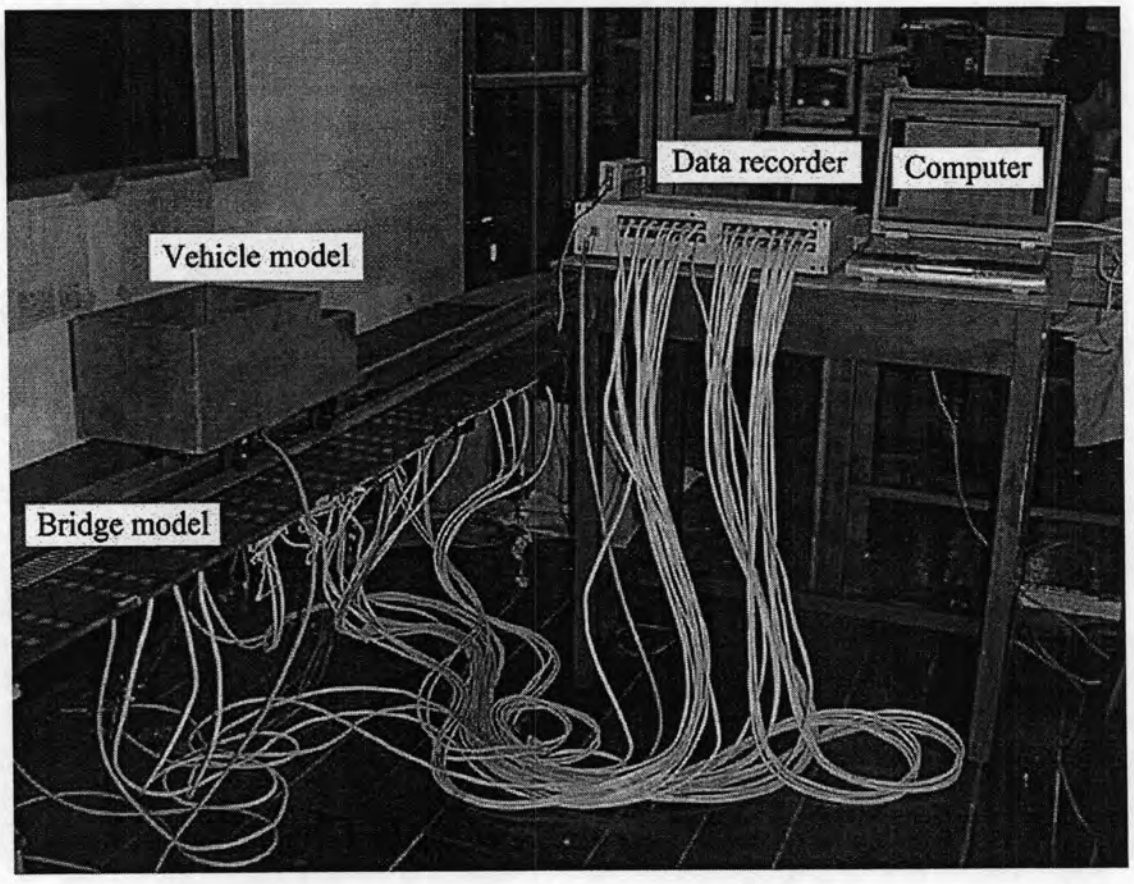

Figure 5.1(d) Photograph of the experimental test

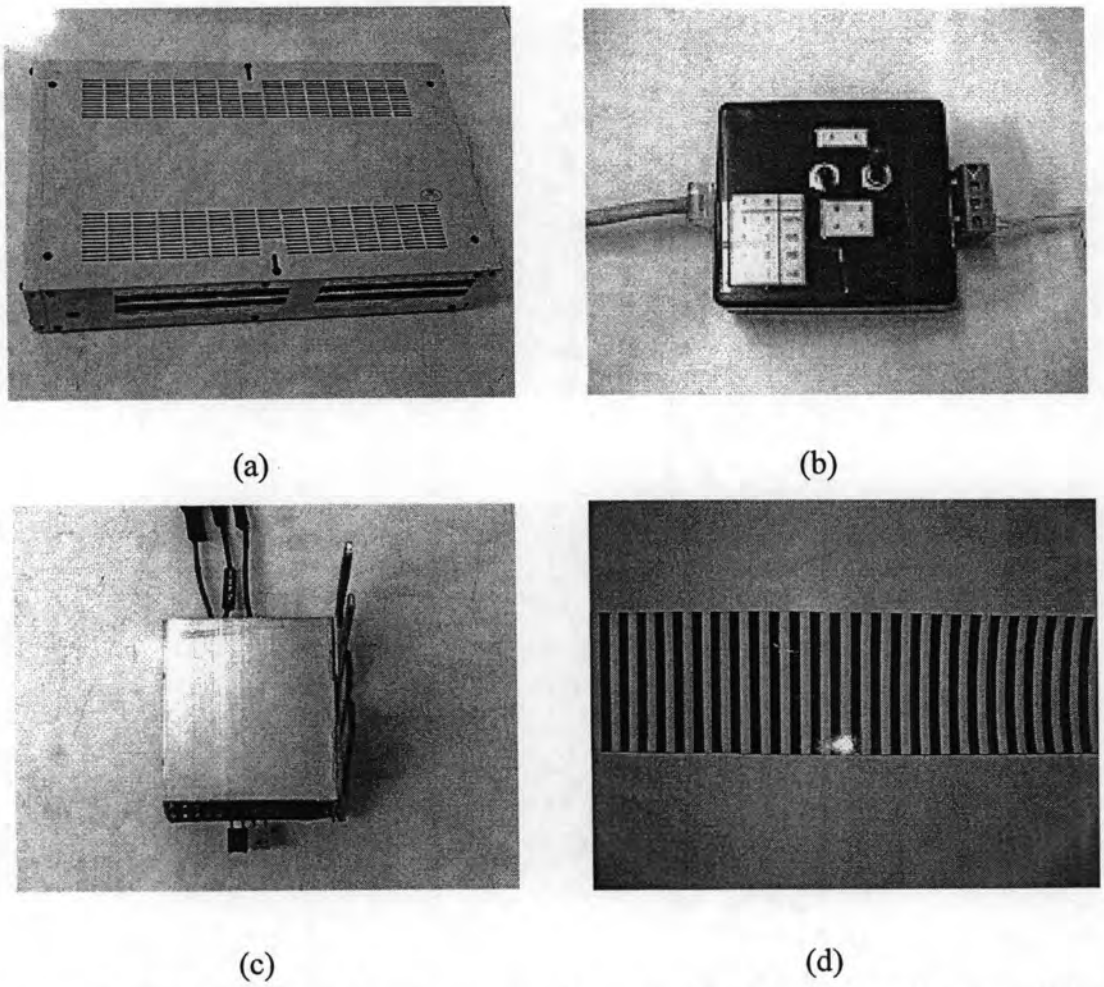

(a) (b)

(c) (d)

Figure 5.2 Photographs of instruments used in experimental test: (a) 48-channel data logger, (b) completion bridge box, (c) optical sensor, (d) black/white stripes

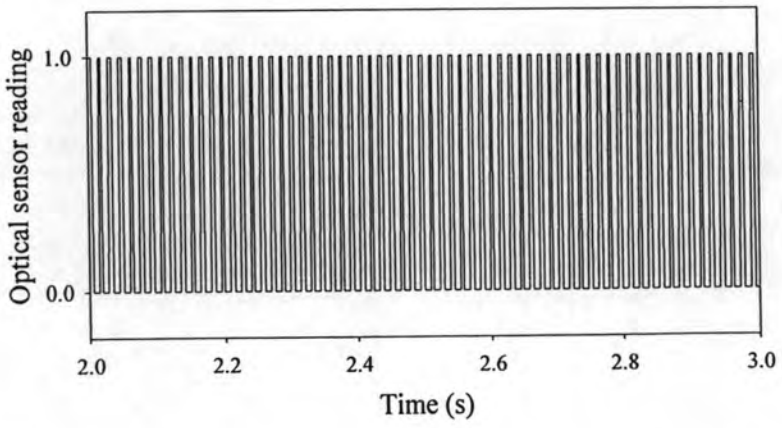

Figure 5.3 Typical measured signal of the optical sensor reading used for vehicle's position measurement

5.3 Strains and Bending Moments of the Bridge

The effect of bridge torsion on the strain readings is firstly investigated. The typical measured signals from the nine strains at the *L*/2 section for the case of a vehicle with 300 N weight moving at a moderate speed of 45 cm/s on the bridge in left, middle and right lanes are plotted in Figures 5.4(a) to 5.4(c), respectively. Based on those strains, the strain distributions across the bridge section, when the distance of front axle of the vehicle is about 130 cm, are extracted and plotted in Figure 5.5. It is observed that the strain values across the bridge section are significantly affected by the transverse positions of the vehicle. Consequently, the direct use of the bridge strains as the input for axle loads identification would require the 3-D bridge model to accurately simulate the torsion effect (Law et al., 2007). However, to simplify the identification procedure the equivalent 2-D bridge model is preferred. The bending moments of the bridge are employed for loads identification instead of the bridge strains. It should be noted that, using these bending moments as the input for loads identifications, the effect of bridge torsion induced by the off-center line loading can be eliminated. To monitor the bridge bending moments of the actual bridge system, the strain gauges are uniformly attached beneath the deck across the bridge section as shown in Figure 5.1(a), then, the bending moments are assumed to be constructed from the weighted summation of those measured strain readings ε_i of that bridge section as

$$m_j(t) = \sum_{i=1}^{NS} \left(\frac{EI_i}{\xi} \varepsilon_i(t) \right)_j \tag{5.1}$$

where ξ is the distance between the bottom fiber and the neutral axis, and I_i is the effective moment inertia of the section for a small portion i while NS is the total number of the strain gauges in the section.

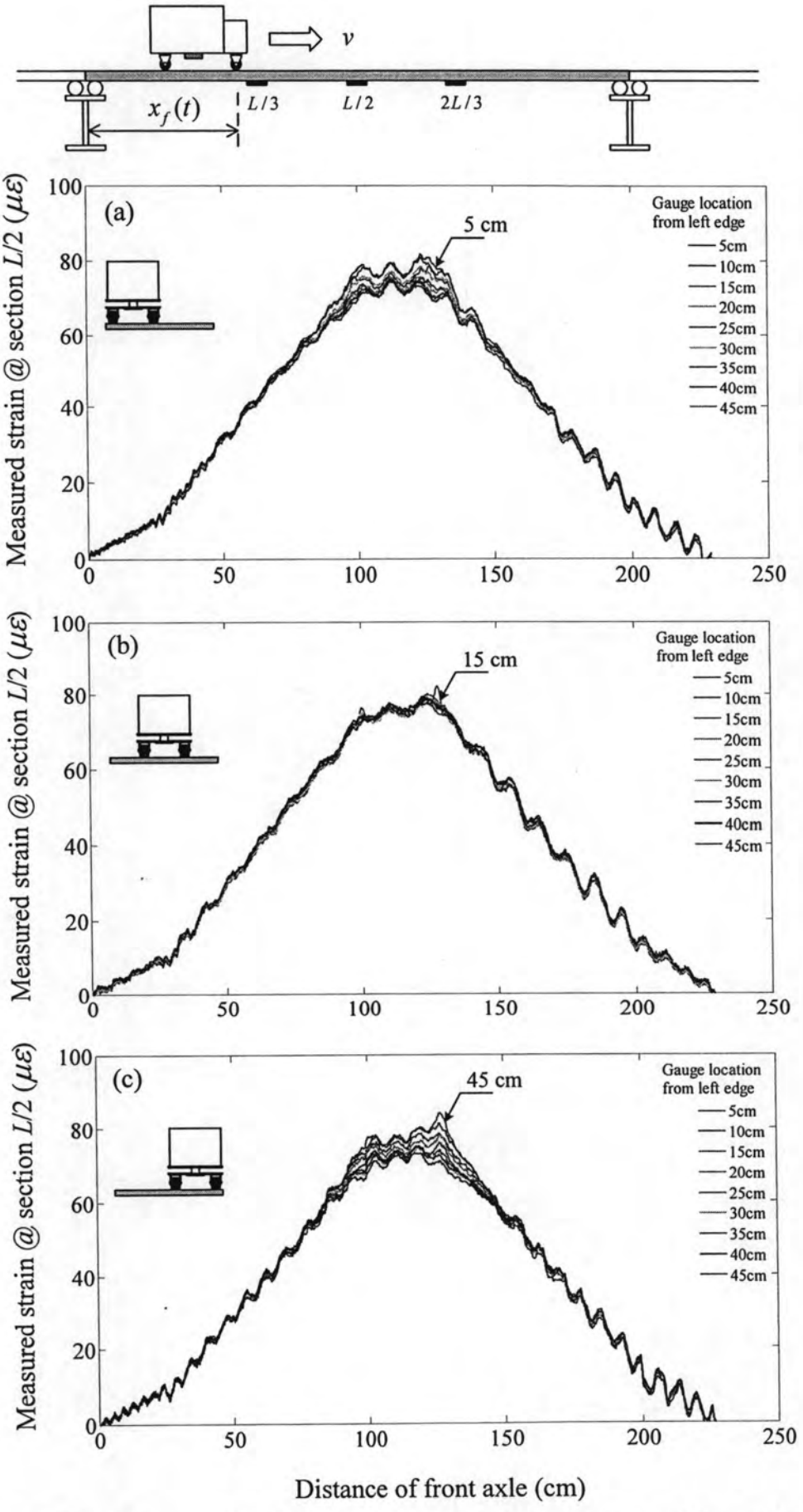

Figure 5.4 Typical measured strains at section $L/2$ under various travelling paths of a vehicle: (a) left lane and (b) middle lane and (c) right lane

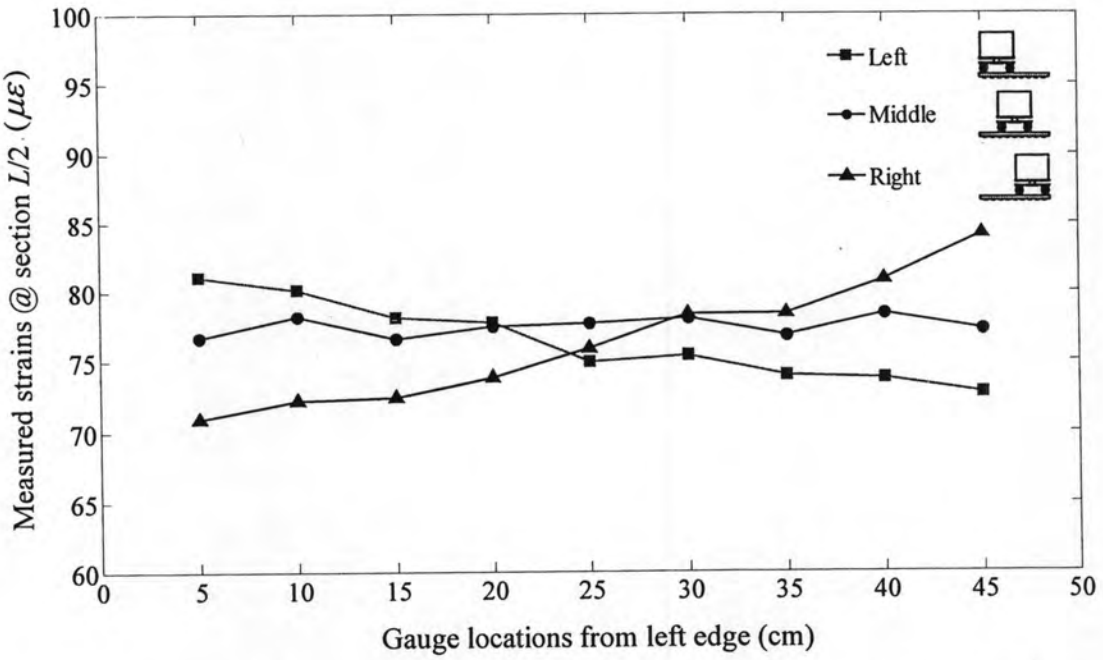

Figure 5.5 Typical measured strain distributions across section $L/2$ under various travelling paths of vehicle

The typical computed bending moments of the bridge under a vehicle moving on the left, right and middle lane at sections $L/3$, $L/2$ and $2L/3$ are shown in Figures 5.6(a) to 5.6(c), respectively. It is clearly observed from the figures that the bridge moments are not affected by the transverse positions of the vehicle and its use with a 2-D bridge model for axle load identifications should be acceptable. Moreover, these figures demonstrate that the continuity effect from the side spans on bending moments of the bridge is perfectly zero. Therefore, the bridge can be considered as a simply supported beam.

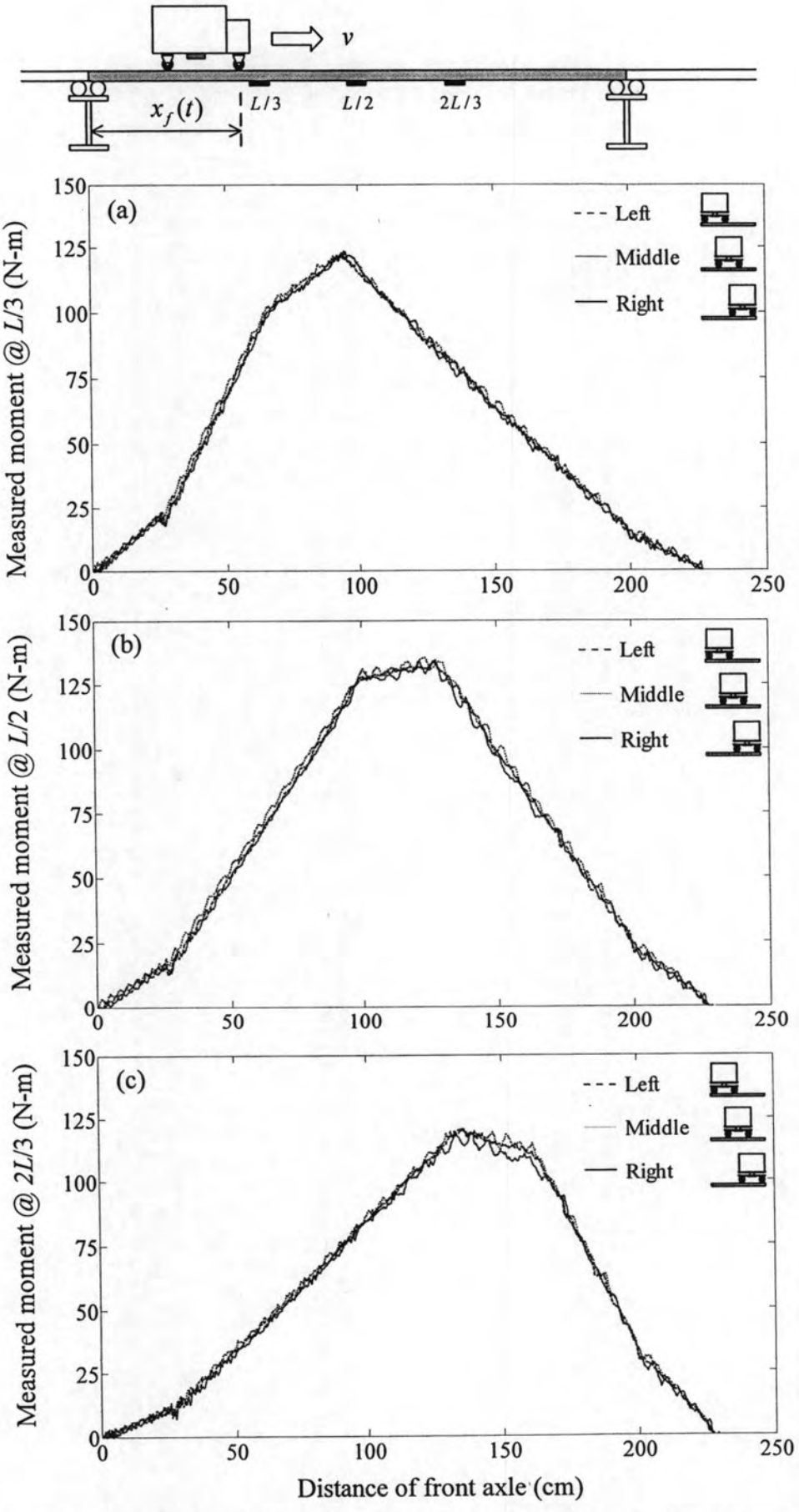

Figure 5.6 Typical measured bending moments (**Z**) of bridge under various travelling paths of vehicle at sections: (a) $L/3$ (b) $L/2$ and (c) $2L/3$

5.4 Axle Weight Estimations

In the following, the effectiveness of the two identification methods is investigated via the experimental tests. The experiments were conducted for various vehicle weights, speeds and travelling paths. The identification accuracies obtained from Method I and Method II are examined and compared. Approximately 27 different conditions of passing vehicles are considered. During the passage of the vehicle, the bending moments of the bridge at three sections, i.e. $L/3$, $L/2$ and $2L/3$ as well as the positions of the vehicle are measured and are used as the inputs for vehicle weight identifications. The identification utilizes the vehicle-bridge model outlined in previous sections. The model is calibrated by adjusting the section modulus of the bridge so that predicted bridge strains at the mid-span section match the corresponding strains obtained from the measurement under a static placement of a test vehicle at the bridge mid-span.

A vehicle weight of 100, 200 and 300 N and vehicle speeds ranging from 10 to 120 cm/s and three travelling paths: left, middle and right of the bridge are investigated. Taking the speed variation into account, the average speeds of the vehicle between 10-20 cm/s, 40-60 cm/s and 90-120 cm/s are denoted as the slow, moderate and fast speed levels, respectively. For each speed level, weight and traveling path, the experiments are conducted for three runs. Figures 5.7(a) and 5.7(b) show the front and rear dynamic axle load of a vehicle from measurement and results identified by Method I and Method II when the vehicle with weight of 300 N moving at 45cm/s speed on the middle-lane of the bridge. It should be noted that Method I yields directly the two constant axle weights of the vehicle. While method II firstly yields the time-varying magnitudes of dynamic axle loads which, consequently, can be averaged to estimate the corresponding axle weights of the vehicle. The parameter for the regularization method with USC is found to be much less sensitive and can be fixed to any number from 0.001 to 10. However, for simplicity, the value of 0.1 is employed throughout this experimental investigation.

5.4.1 Effect of Vehicle Weight and Moving Speed

Figures 5.8(a) and 5.8(b) present the average estimation errors of the obtained axle weights under various vehicle weights and moving speeds identified by Method I and Method II, respectively. From the figures, the axle weight estimation errors are not clearly affected by the vehicle weights and vehicle moving speeds. Although the

numerical simulation shows the vehicle speed has strong influence on weight estimation it is shown from experimental investigation that the errors are not significantly affected by the vehicle speeds in the range of 10 – 120 cm/s which are compared with 0.5 m/sec to 10 m/sec in the numerical simulation. These speed ranges are not higher than speed ranges in numerical simulation which affect the accuracy of axle weight estimation (vehicle speed >20m/sec). This is because the vehicle speeds in the experimental test did not significantly affect the accuracy of axle weight estimation methods.

5.4.2 Effect of Travelling Paths of Vehicle

The effect of travelling paths of the vehicle is investigated in the experimental test. The three transverse vehicle travelling paths are 1) on the bridge center line; 2) 12.5 cm from the left edge of the bridge; and 3) 12.5 cm from the right edge of the bridge. Figure 5.9(a) and 5.9(b) present the average estimation errors of the obtained axle weights under various vehicle weights and travelling paths obtained from Method I and Method II, respectively. The results indicate that the axle weight estimation errors are not strongly affected by vehicle travelling paths. In particular, it is observed that the estimation errors of all cases are well below 10% for both methods. Therefore, using the average sectional bending moments, converted from strain readings distributed in each bridge section, as the input for weight estimation seems sufficient and effective.

5.4.3 Effectiveness of Estimation Methods

Based on 27 conditions of passing vehicles with 81 runs of tests, Table 5.1 list the estimation errors of the axle weight from Method I and Method II. The statistical values of the obtained results are listed in Table 5.2. It is obvious from the table that the two methods provide quite accurate weight estimations of the vehicle, i.e. errors < ±6%, in almost of all cases. From the tables, the axle weight estimation errors are not clearly affected by the vehicle masses, speeds or its travelling paths. It is also found that the accuracy of estimation method is not affected by using the average sectional bending moment concept. This concept can be effectively used for both axle weight estimation methods. Comparing the two methods, it is observed that Method I is slightly better than Method II. However, the obtained results from both methods show that the accuracy level of the WIM system of type-III can be experimentally achieved.

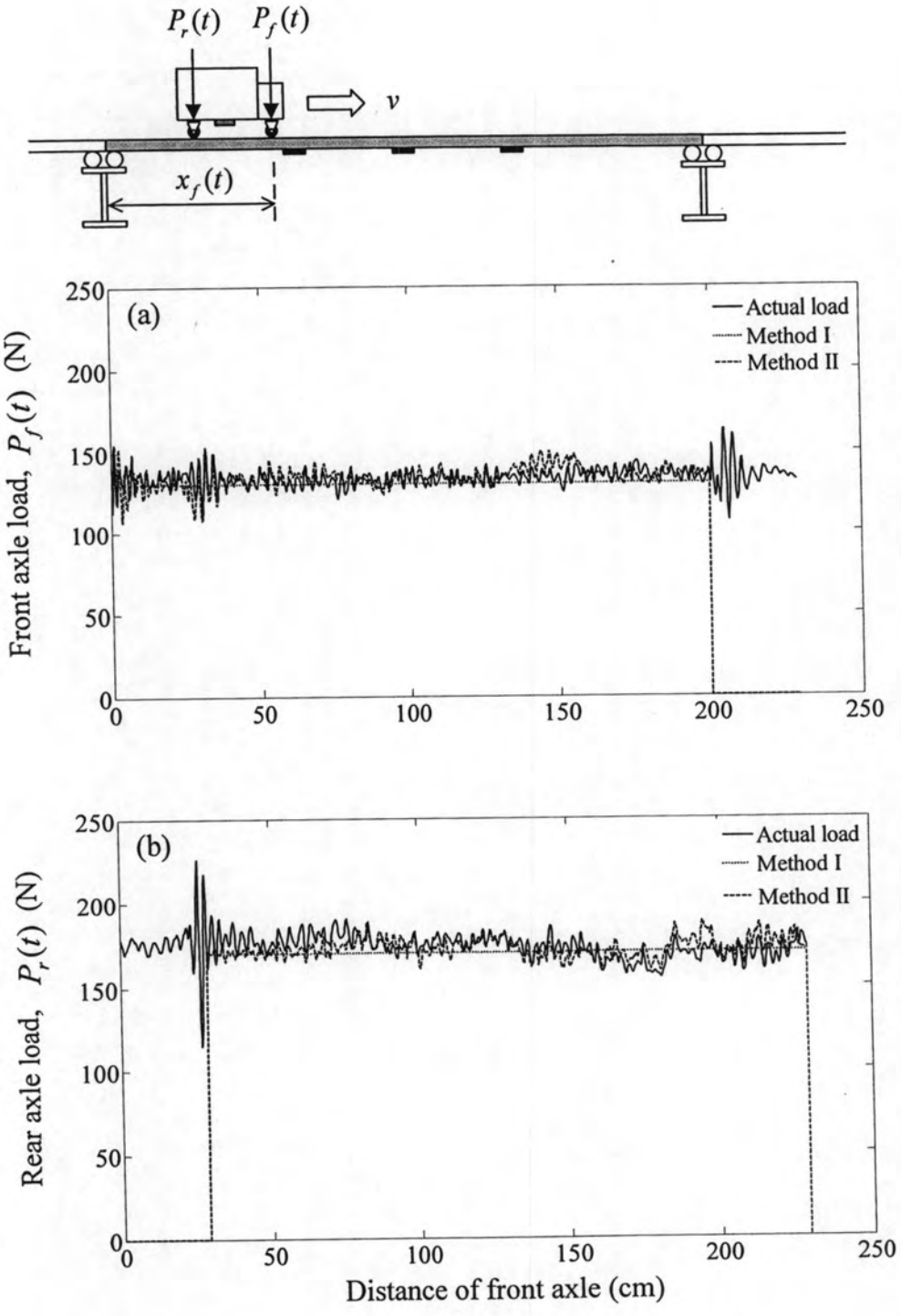

Figure 5.7 Identification results of axle loads of vehicle for, (a) front axle, (b) rear axle

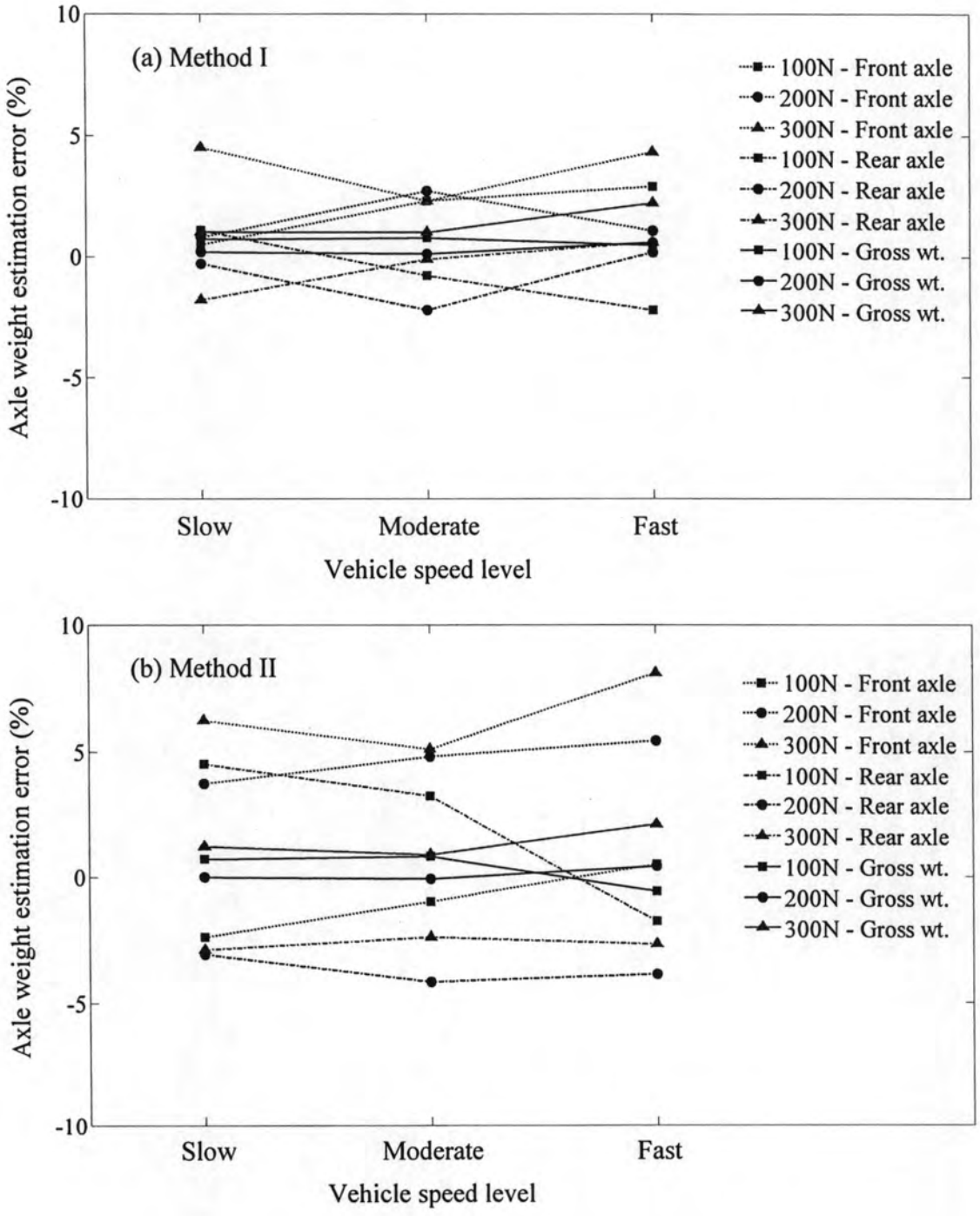

Figure 5.8 Estimation errors of axle weights under various vehicle weights and vehicle speeds using (a) Method I and (b) Method II

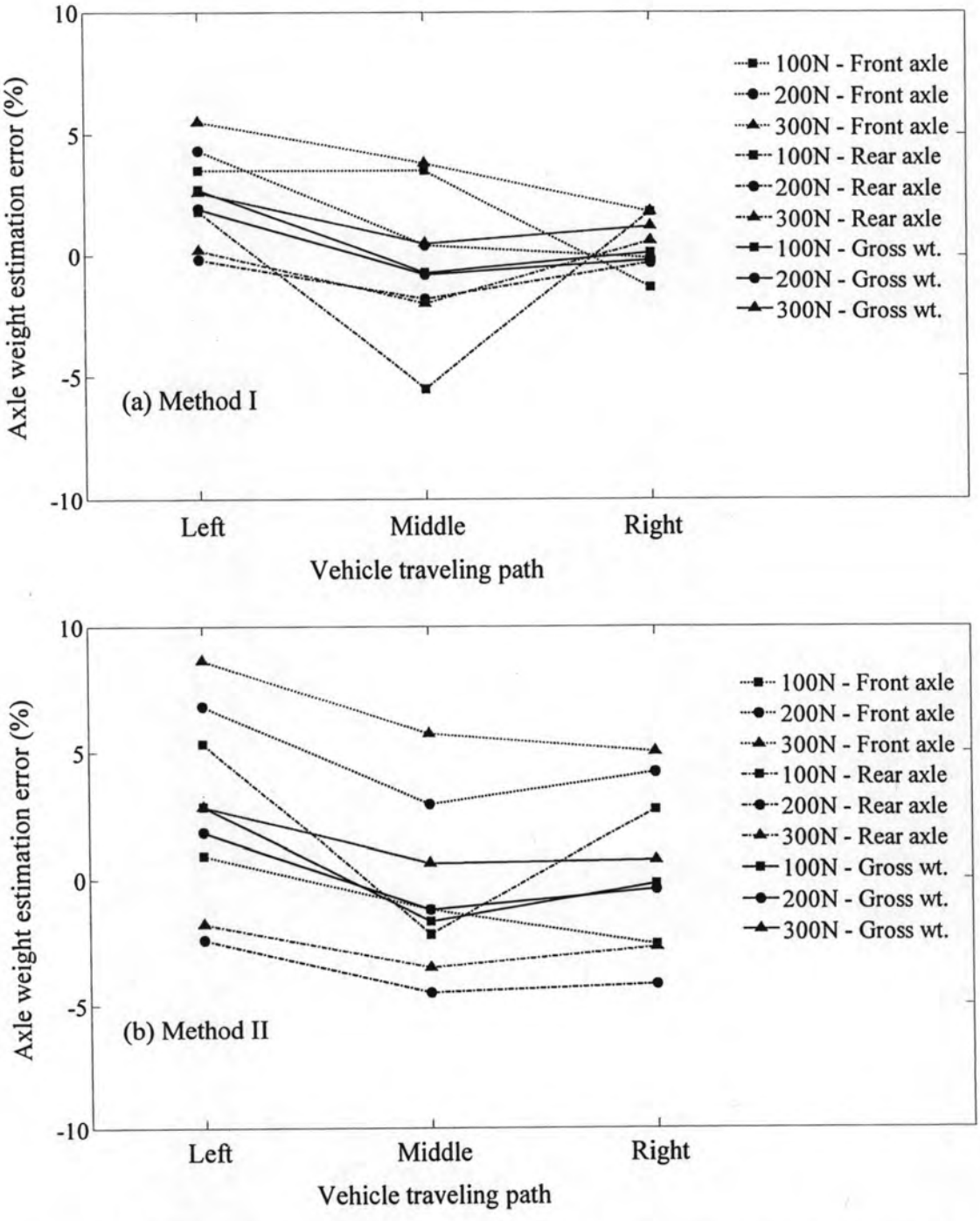

Figure 5.9 Estimation errors of axle weights under various vehicle weights and vehicle travelling paths using (a) Method I and (b) Method II

Table 5.1 Estimation errors of axle weights using Method I and Method II

Vehicle Weight (N)	Speed (cm/s)	Estimation error (%)	Left Test number 1	2	3	Average	Middle Test number 1	2	3	Average	Right Test number 1	2	3	Average
		Front axle	3.4	2.3	3.5	**3.0**	3.2	1.1	1.4	**1.9**	-4.9	-2.8	-2.6	**-3.4**
			(0.0)	(1.0)	(-0.3)	**(0.2)**	(-1.7)	(-4.4)	(-3.6)	**(-3.2)**	(-4.5)	(-4.0)	(-3.6)	**(-4.0)**
	Slow	rear axle	3.2	2.9	2.1	**2.7**	-5.7	-3.5	-4.8	**-4.6**	7.7	4.1	3.8	**5.2**
	(10-20)		(8.2)	(6.8)	(7.4)	**(7.5)**	(-0.4)	(-2.0)	(0.1)	**(0.6)**	(6.5)	(4.9)	(4.7)	**(5.4)**
		Gross wt.	3.2	2.5	2.8	**2.8**	-0.9	-1.0	-1.5	**-1.1**	0.8	0.3	0.2	**0.5**
			(3.7)	(3.6)	(3.1)	**(3.5)**	(-1.2)	(-1.6)	(-2.0)	**(-1.6)**	(0.4)	(0.0)	(0.1)	**(0.2)**
		Front axle	4.7	5.2	3.9	**4.6**	3.6	3.1	6.3	**4.3**	-1.5	-3.2	-1.5	**-2.1**
100			(1.1)	(2.9)	(1.1)	**(1.7)**	(-1.0)	(-3.5)	(1.0)	**(-1.2)**	(-3.4)	(-3.9)	(-3.7)	**(-3.6)**
	Moderate	rear axle	1.0	0.8	0.9	**0.9**	-2.1	-6.7	-4.2	**-4.3**	1.5	2.1	-0.2	**1.1**
	(40-60)		(6.3)	(4.5)	(4.8)	**(5.2)**	(2.9)	(-0.3)	(2.6)	**(1.7)**	(3.2)	(2.4)	(2.2)	**(2.6)**
		Gross wt.	3.0	3.1	2.5	**2.8**	1.0	-1.4	1.4	**0.3**	-0.2	-0.8	-1.0	**-0.7**
			(3.4)	(3.6)	(2.7)	**(3.2)**	(0.7)	(-2.1)	(1.7)	**(0.1)**	(-0.5)	(-1.1)	(-1.1)	**(-0.9)**
		Front axle	9.7	-1.3	0.4	**2.9**	5.8	8.5	-1.9	**4.1**	1.8	1.6	1.6	**1.7**
			(4.6)	(-1.2)	(-0.9)	**(0.8)**	(3.4)	(5.6)	(-6.4)	**(0.9)**	(-0.4)	(-0.1)	(0.4)	**(0.0)**
	Fast	rear axle	-5.7	6.4	4.8	**1.8**	-5.4	-12.3	-4.9	**-7.6**	0.9	-4.5	0.6	**-1.0**
	(90-120)		(-2.7)	(6.9)	(5.4)	**(3.2)**	(-5.5)	(-13.4)	(-7.5)	**(8.8)**	(1.7)	(-3.4)	(2.5)	**(0.3)**
		Gross wt.	2.6	2.1	2.3	**2.4**	0.6	-1.0	-3.4	**-1.3**	1.3	-1.2	1.1	**0.4**
			(1.2)	(2.4)	(1.9)	**(1.8)**	(-0.7)	(-3.1)	(-6.9)	**(-3.6)**	(0.5)	(-1.7)	(1.3)	**(0.0)**
		Front axle	4.7	3.7	2.6	**3.7**	-0.1	1.0	-0.3	**0.2**	-1.8	-1.9	-0.7	**-1.4**
			(6.5)	(5.8)	(6.6)	**(6.3)**	(2.2)	(0.0)	(2.3)	**(1.5)**	(3.2)	(2.5)	(4.0)	**(3.2)**
	Slow	rear axle	0.8	0.6	2.0	**1.1**	-1.2	-3.7	-1.4	**-2.1**	0.2	-0.4	0.3	**0.0**
	(10-20)		(-0.8)	(-1.2)	(-0.8)	**(-0.9)**	(-3.9)	(-5.0)	(-4.9)	**(-4.6)**	(-3.8)	(-4.3)	(-3.3)	**(-3.8)**
		Gross wt.	2.6	2.0	2.2	**2.3**	-0.7	-1.6	-0.9	**-1.1**	-0.7	-1.1	-0.1	**-0.6**
			(2.5)	(2.0)	(2.5)	**(2.4)**	(-1.1)	(-2.7)	(-1.6)	**(-1.8)**	(-0.6)	(-1.2)	(0.0)	**(-0.6)**
		Front axle	4.7	3.9	3.8	**4.2**	2.2	0.2	4.0	**2.1**	2.2	2.3	1.0	**1.8**
200			(7.5)	(5.9)	(6.1)	**(6.5)**	(4.4)	(2.2)	(4.6)	**(3.7)**	(4.0)	(4.4)	(3.8)	**(4.1)**
	Moderate	rear axle	-0.4	-0.8	-0.2	**-0.5**	-2.9	-0.7	-4.8	**-2.8**	-3.5	-2.8	-3.4	**-3.2**
	(40-60)		(-2.6)	(-2.8)	(-2.1)	**(-2.5)**	(-4.6)	(-2.8)	(-6.2)	**(-4.5)**	(-5.7)	(5.1)	(-6.1)	**(-5.6)**
		Gross wt.	1.9	1.4	1.6	**1.6**	-0.5	-0.3	-0.8	**-0.5**	-0.9	-0.5	-1.4	**-0.9**
			(2.0)	(1.1)	(1.7)	**(1.6)**	(-0.5)	(-0.5)	(-1.3)	**(-0.8)**	(-1.3)	(-0.8)	(-1.6)	**(-1.2)**
		Front axle	3.9	5.9	5.8	**5.2**	-3.1	-3.6	3.4	**-1.1**	-0.3	-2.1	0.2	**-0.7**
			(7.5)	(7.5)	(8.0)	**(7.6)**	(2.7)	(1.6)	(5.7)	**(3.3)**	(5.6)	(5.1)	(5.3)	**(5.3)**
	Fast	rear axle	1.3	-2.9	-1.7	**-1.1**	1.6	1.4	-4.9	**-0.6**	2.7	4.8	-0.6	**2.3**
	(90-120)		(-1.9)	(-5.7)	(-4.0)	**(-3.9)**	(-3.1)	(-3.5)	(-6.9)	**(-4.5)**	(-2.1)	(-2.2)	(-5.6)	**(-3.3)**
		Gross wt.	2.5	1.1	1.7	**1.8**	-0.5	-0.9	-1.1	**-0.8**	1.3	1.7	-0.2	**0.9**
			(2.4)	(0.3)	(1.5)	**(1.4)**	(-0.5)	(-1.1)	(-1.1)	**(-0.9)**	(1.4)	(1.1)	(-0.6)	**(0.7)**
		Front axle	6.1	4.6	6.5	**5.8**	4.9	5.6	6.5	**5.6**	3.1	1.8	1.4	**2.1**
			(9.6)	(8.5)	(10.1)	**(9.4)**	(5.1)	(1.5)	(7.4)	**(4.7)**	(4.9)	(4.7)	(4.4)	**(4.7)**
	Slow	rear axle	-0.4	0.7	-1.3	**-0.4**	-4.2	-5.7	-4.7	**-4.9**	-1.6	0.8	0.4	**-0.1**
	(10-20)		(-2.5)	(-1.3)	(-3.3)	**(-2.4)**	(-5.3)	(-2.2)	(-3.4)	**(-3.6)**	(-4.0)	(-1.8)	(2.3)	**(-2.7)**
		Gross wt.	2.5	2.4	2.2	**2.4**	-0.1	-0.7	0.3	**-0.2**	0.5	1.2	0.8	**0.9**
			(2.9)	(3.1)	(2.6)	**(2.9)**	(-0.7)	(-0.5)	(1.4)	**(0.1)**	(0.0)	(1.1)	(0.7)	**(0.6)**
		Front axle	-0.7	8.4	4.9	**4.2**	0.7	6.8	-0.4	**2.4**	3.7	-3.5	1.2	**0.5**
300			(4.2)	(8.6)	(7.8)	**(6.9)**	(4.3)	(7.4)	(3.1)	**(4.9)**	(6.3)	(1.3)	(2.5)	**(3.4)**
	Moderate	rear axle	4.0	-5.9	-1.2	**-1.0**	1.5	-5.1	3.5	**-0.1**	-0.9	4.9	-1.4	**0.9**
	(40-60)		(1.0)	(-6.1)	(-3.0)	**(-2.7)**	(-1.7)	(-5.8)	(0.2)	**(-2.4)**	(-3.6)	(1.0)	(-3.6)	**(-2.1)**
		Gross wt.	1.9	0.5	1.5	**1.3**	1.1	0.2	1.7	**1.0**	1.2	1.1	-0.3	**0.7**
			(2.4)	(0.4)	(1.8)	**(1.6)**	(1.0)	(0.1)	(1.5)	**(0.9)**	(0.8)	(1.1)	(-0.9)	**(0.4)**
		Front axle	6.5	6.6	6.6	**6.6**	4.6	0.0	5.3	**3.3**	2.2	2.3	4.0	**2.8**
			(10.3)	(12.2)	(6.4)	**(9.6)**	(8.3)	(5.3)	(8.9)	**(7.5)**	(6.8)	(7.0)	(7.4)	**(7.1)**
	Fast	rear axle	2.7	1.6	1.6	**2.0**	-3.4	2.2	-2.5	**-1.2**	3.4	1.3	-1.1	**1.2**
	(90-120)		(-0.4)	(-2.8)	(2.2)	**(-0.3)**	(-6.1)	(-1.7)	(-5.4)	**(-4.4)**	(-1.6)	(-3.7)	(-5.0)	**(-3.4)**
		Gross wt.	4.4	3.9	3.9	**4.0**	0.1	1.2	1.0	**0.8**	2.9	1.7	1.2	**1.9**
			(4.4)	(3.9)	(4.0)	**(4.1)**	(0.3)	(1.4)	(1.0)	**(0.9)**	(2.1)	(1.1	(0.5)	**(1.2)**

Remark: The numbers in the brackets (.) are the estimation errors from Method II.

Table 5.2 Statistical values of axle weight estimation errors using Method I and Method II

Method	Weight	Min (%)	Max (%)	Mean (%)	SD
I	Front Axle	-4.9	9.7	2.4	3.2
	Rear Axle	-12.3	7.7	-0.6	3.5
	Gross weight	-3.4	4.4	0.8	1.5
II	Front Axle	-6.4	12.2	3.4	4.1
	Rear Axle	-13.4	8.2	-1.5	4.1
	Gross weight	-6.9	4.4	0.6	1.9

5.5 Dynamic Axle Loads Identification

Since Method II provides not only the estimated axle weight of the vehicle but also its dynamic axle loads, it is therefore interesting to investigate the accuracy of the identified dynamic axle loads. To do so, the dynamic load identification errors of front and rear axles as defined in Eq. (3.86) are examined. The regularization parameter is simply fixed at 0.1. Based on these 27 conditions of passing vehicles with 81 runs of tests, the effects of vehicle weight, moving speed and travelling path are considered.

5.5.1 Effect of the Vehicle Weight and Moving Speed

Figures 5.10 presents the average identification errors of the obtained axle loads under various vehicle weights and moving speeds identified from Method II. From the test results, the axle weight identification errors are clearly affected by the vehicle weight and the vehicle moving speed. This is because the vehicle with lower speed induces less dynamic interaction with the bridge. In addition, a heavier vehicle normally induces a lager signal to noise ratio than a lighter vehicle, therefore, the collected response with smaller dynamic fluctuation and larger signal to noise ratio usually provides a more accurate identification than one with larger dynamic fluctuation and smaller signal to noise ratio. Comparing between these two parameters, it is also observed that the vehicle moving speed has stronger influence on the identification accuracy than the vehicle weight.

5.5.2 Effect of Travelling Paths of Vehicle

The effect of travelling paths of the vehicle is experimentally investigated. The three transverse vehicle travelling paths are 1) on the bridge center line; 2) 12.5 cm from the left edge of the bridge; and 3) 12.5 cm from the right edge of the bridge. Figure 5.11 presents the average identification errors of the obtained axle loads under various vehicle weights and travelling paths identified from Method II. The results indicate that the axle load identification errors are not clearly affected by vehicle travelling paths. In particular, it is observed that the average identification errors of all cases are below 15%. Therefore, using the average sectional bending moments, converted from strain readings distributed in each bridge section, as the input for dynamic axle loads identification seems sufficient and effective.

5.5.3 Effectiveness of the Identification Method

Based on 27 conditions of passing vehicles with 81 runs of tests, Table 5.3 lists the identification errors of axle loads from Method II. It is found from the table that the errors are affected by the vehicle weight and speed. Obviously, the identification errors of dynamic front and rear axle loads increase as the vehicle speed increases. This is because the load identification is based on the minimization of the bending moments of the bridge which usually contain only the low frequency signals close to the bridge natural frequencies. Therefore, the high frequency axle loads resulting from the fast speed vehicle are difficult to be identified. It is also noticed from the table that the identification errors of both axle loads tend to be decreased as the vehicle weight increases. This is because the ratio of the load fluctuation to the weight of the axle is reduced when the vehicle weight increases. For the effect of vehicle travelling paths, it is observed that the accuracy of the identification method is not significantly affected.

5.6 Summary

The effectiveness of the vehicle weight estimations is investigation through small-scale tests. The measured bending moments of the simply-supported bridge at selected sections under a passage of the vehicle are used as the input for the vehicle weight estimations. Two axle weight estimation methods assuming constant magnitudes (Method I) and time-varying magnitudes (Method II) of the vehicle axle

loads are investigated. Their estimation accuracy are evaluated and compared under various conditions of passing vehicles.

From the small-scale test results, it is found that the truck weights, speeds and transverse travelling paths are not clearly affected the accuracy of the both estimation methods. It is also found that the accuracy of estimation method is not affected by using the average sectional bending moment concept. This concept can be effectively used for both axle weight estimation methods. Comparing the two methods, it is observed that Method I is slightly better than Method II. However, the obtained results from both methods show that the accuracy level of the WIM system of type-III (errors $< \pm 6\%$, in almost of all cases) can be experimentally achieved.

Based on the dynamic axle loads identification results using Method II, the axle weight identification errors are clearly affected by the vehicle weight and the vehicle moving speed. Comparing between these two parameters, it is also observed that the vehicle moving speed has stronger influence on the identification accuracy than the vehicle weight. For the effect of vehicle travelling paths, it is observed that the accuracy of the identification method is not significantly affected by using the average sectional bending moment concept.

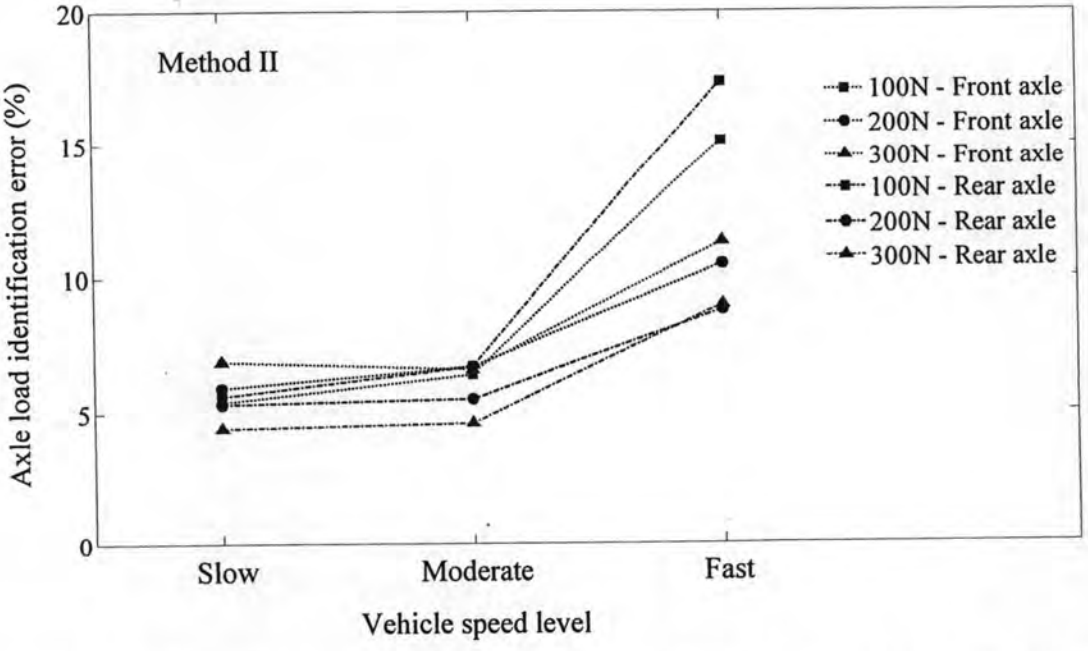

Figure 5.10 Identification errors of axle loads under various vehicle weights and vehicle moving speeds using Method II

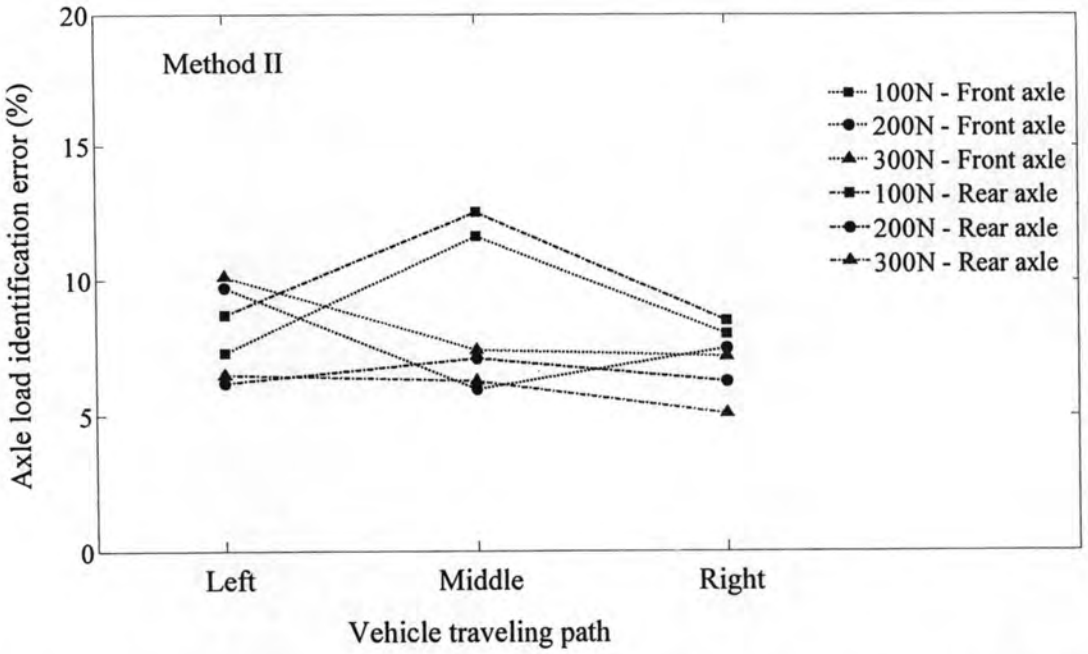

Figure 5.11 Identification errors of axle loads under various vehicle weights and vehicle travelling paths using Method II

Table 5.3 Identification errors of axle loads using Method II

Vehicle weight (N)	Speed (cm/sec)	Iden. error (%)	Left Test number 1	2	3	Average	Middle Test number 1	2	3	Average	Right Test number 1	2	3	Average
100	Slow	Front axle	3.7	3.8	3.5	**3.7**	6.8	8.1	8.9	**7.9**	4.3	3.8	6.0	**4.7**
		Rear axle	5.9	5.8	5.9	**5.9**	3.9	6.3	5.1	**5.1**	4.6	7.4	5.9	**6.0**
	Moderate	Front axle	6.0	5.3	5.0	**5.4**	9.7	6.5	6.2	**7.5**	7.2	5.7	5.8	**6.2**
		Rear axle	5.9	5.6	6.1	**5.9**	7.3	8.1	8.9	**8.1**	6.1	5.8	6.7	**6.2**
	Fast	Front axle	14.1	12.0	12.1	**12.7**	16.6	20.4	21.3	**19.5**	14.3	12.5	12.6	**13.1**
		Rear axle	14.7	13.8	14.3	**14.2**	21.0	27.5	24.5	**24.3**	10.7	14.8	14.8	**13.4**
200	Slow	Front axle	8.0	7.0	8.2	**7.7**	4.3	3.3	4.3	**4.0**	6.1	5.9	5.9	**6.0**
		Rear axle	3.7	4.1	4.8	**4.2**	6.0	6.5	6.5	**6.4**	5.2	5.9	5.1	**5.4**
	Moderate	Front axle	8.9	7.4	7.1	**7.8**	5.3	5.8	6.5	**5.9**	6.3	6.9	6.2	**6.5**
		Rear axle	3.8	6.0	4.4	**4.7**	5.5	7.0	6.3	**6.3**	5.8	5.6	5.2	**5.5**
	Fast	Front axle	13.0	13.2	14.0	**13.4**	7.8	8.6	7.7	**8.0**	10.9	9.0	10.4	**10.1**
		Rear axle	8.9	9.9	10.3	**9.7**	8.3	8.1	9.3	**8.5**	8.2	8.0	8.1	**8.1**
300	Slow	Front axle	10.0	10.2	10.1	**10.1**	5.1	5.8	3.0	**4.6**	6.0	5.8	5.5	**5.8**
		Rear axle	4.7	4.5	4.5	**4.6**	4.8	5.8	3.9	**4.8**	4.0	3.7	3.4	**3.7**
	Moderate	Front axle	6.0	8.9	7.9	**7.6**	5.9	10.0	5.5	**7.1**	6.4	4.2	4.9	**5.2**
		Rear axle	4.8	4.6	4.2	**4.5**	4.5	5.5	5.3	**5.1**	4.6	3.9	3.5	**4.0**
	Fast	Front axle	13.0	13.6	11.5	**12.7**	11.2	11.7	8.7	**10.5**	11.4	10.7	10.0	**10.7**
		Rear axle	11.9	9.2	9.9	**10.3**	7.0	8.6	11.6	**9.1**	6.9	7.6	7.8	**7.4**